

Clinical significance for diagnosis and prognosis of POP1 and its potential role in breast cancer: a comprehensive analysis based on multiple databases

Xiao He^{1,*}, Ji Wang^{2,*}, Honghao Yu¹, Wenchang Lv¹, Yichen Wang¹, Qi Zhang¹, Zeming Liu¹, Yiping Wu¹

¹Department of Plastic Surgery, Tongji Hospital, Tongji Medical College, Huazhong University of Science and Technology, Wuhan 430030, Hubei, China

²Department of Emergency, The People's Hospital of China Three Gorges University, The First People's Hospital of Yichang, Yichang 443000, Hubei, China

*Equal contribution and first co-authors

Correspondence to: Qi Zhang, Zeming Liu, Yiping Wu; **email:** zhangqi06172@foxmail.com, <https://orcid.org/0000-0003-0564-9215>; 6myt@163.com, <https://orcid.org/0000-0001-6132-4701>; tongjiplastic@163.com, <https://orcid.org/0000-0002-4815-0732>

Keywords: breast cancer, bioinformatics, The Cancer Genome Atlas, Gene Expression Omnibus, POP1

Received: May 7, 2022

Accepted: August 17, 2022

Published: September 9, 2022

Copyright: © 2022 He et al. This is an open access article distributed under the terms of the [Creative Commons Attribution License](https://creativecommons.org/licenses/by/3.0/) (CC BY 3.0), which permits unrestricted use, distribution, and reproduction in any medium, provided the original author and source are credited.

ABSTRACT

Background: Breast cancer (BC) is one of the most common cancers in women. The discovery of available biomarkers is crucial for early diagnosis and improving prognosis. The effect of POP1 in BC remains unrevealed. Our study aims to explore the expression of POP1 in BC and demonstrate its clinical significance and potential molecular mechanisms.

Methods: The Cancer Genome Atlas (TCGA) BC cohort transcriptome data and corresponding clinical information were downloaded. GSE42568 cohort, GSE162228 cohort, GSE7904 cohort, and GSE161533 cohort in the Gene Expression Omnibus (GEO) database were used as verification groups. R software and several web tools were used for statistical analysis. Moreover, the proliferation, transwell, wound healing experiments, and flow cytometry were used for *in vitro* investigation.

Results: Compared with normal breast tissue, POP1 expression was up-regulated in BC tissue with a higher mutation rate. POP1 had good diagnostic value for BC and could be utilized as a new marker. POP1 was significantly correlated with multiple pathways in BC and played an important role in the immune infiltration of BC. High-POP1 expression patients were more prone to be responded to immunotherapy and had a significantly higher percentage of immunotherapy response rate. Moreover, POP1 promoted proliferation and migration and inhibited apoptosis in BC cells.

Conclusions: POP1 expression was up-regulated in BC and was associated with a poor prognosis. Patients with high-POP1 expression were more likely to be responded to immunotherapy. Our study can provide a potential marker POP1 for BC, which is beneficial in the diagnosis and treatment of BC.

INTRODUCTION

Breast cancer (BC) seriously affects the physical and mental health of women because of its high incidence

[1]. Surgery is still the most common treatment for BC, and other treatments include chemotherapy, radiotherapy, neoadjuvant therapy, targeted therapy, and immunotherapy [2]. With the popularization of

monitoring methods and the development of surgical techniques, early BC patients can get a better prognosis [3]. But, there is still a significant proportion of patients with poor prognoses, such as estrogen receptor (ER)-negative [4, 5]. Although immunotherapy has achieved good outcomes in many solid tumors, its efficacy in BC is limited and only a small percentage of patients can produce a lasting response [6–8]. This may be related to the “cold tumor” feature of BC [9]. Further exploration of potential targets that may be used in BC diagnosis, prognostic monitoring, and efficacy prediction is warranted.

The POP1 gene encodes a ribonuclease that locates in the nucleus and plays a role in tRNA preprocessing [10]. The POP1 protein is also an autoantigen in patients with connective tissue disease and is involved in suppressing inflammation [11, 12]. In recent years, the potential of POP1 has been preliminarily elucidated. For example, Zhu et al. found that POP1 was a novel prognostic marker of colorectal cancer through bioinformatics analysis [13]. Liang et al. constructed a pyroptosis-related prognosis model for gastric cancer, in which POP1 was a gene in the model [14]. However, the role of POP1 in BC has not been intensively investigated.

The relationship between single cells, the microenvironment, and the immune system inside the tumor dictates the progression rate of cancer [15]. Numerous cancers have been ameliorated using immunotherapies such as chimeric antigen receptor (CAR)-T therapy and immune checkpoint blockade (ICB) [16, 17]. Specifically, in renal cell carcinoma, lung adenocarcinoma, and melanoma, antibodies that target immune activation regulators, including programmed cell death protein-1 (PD-1), cytotoxic T-lymphocyte-associated protein 4 (CTLA-4), and programmed death ligand-1 (PD-L1), have significantly increased survival [18]. In recent years, great progress has been made in the treatment of cancer patients with ICBs [19].

Numerous factors generated from cancer cells could regulate the tumor-infiltrating lymphocytes (TILs) response. Immune checkpoints shield tumor cells from immune attacks by inhibiting aberrant activation of TIL response [20]. PD-L1 is a kind of 33 kDa type 1 transmembrane protein, and it can establish a main immune checkpoint via combining with PD-1 on T cells. Therefore, cancer cells can inhibit TILs activation, expansion, and acquisition of effector functions to avoid T cell-mediated immune surveillance [21]. PD-L1 overexpression in solid tumors contributes to the CAR-T cell poor treatment because of mediating the exhaustion of CAR-T cells [22]. Thereby, in the tumor microenvironment (TME), targeting the PD-L1/PD-1

axis might potentially reinvigorate depleted CAR-T cells and TILs [23–25]. However, the response rate for ICB monotherapy is often below 40%, and many patients do not benefit from it [26]. At present, the role of POP1 in anti-tumor immunity is rarely studied. Exploring the relationship between POP1 and the tumor immune microenvironment can contribute to a stronger indicator of tumor status and prediction of treatment response and efficacy.

Bioinformatics analysis provides a convenient and in-depth analytical method to explore the genomics and proteomics of cancer [27]. Gene Expression Omnibus (GEO) database and The Cancer Genome Atlas (TCGA) database are the two most commonly used databases. Their widespread application has led to the successful identification of novel markers and predictive models or signatures for BC. Here, we explored the significance of POP1 in BC through bioinformatics analysis. We combined TCGA data and GEO data sets for comprehensive analysis and validation. Through the analysis of the expression, Kaplan Meier, immune microenvironment, and immune therapy response to explore the role of POP1 in BC. In addition, the Cell Counting Kit-8 (CCK-8) assay, wound healing experiments, transwell, and flow cytometry were applied for in-depth investigations. Our research revealed that POP1 overexpression was correlated with BC poor prognosis and could provide a breakthrough for the clinical diagnosis of BC.

MATERIALS AND METHODS

Expression analysis of POP1 in BC TCGA data and multiple validations in GEO data sets

Firstly, TCGA data was downloaded for analysis. Data sets GSE7904, GSE42568, GSE161533, and GSE162228 in the GEO database were used for validation (Table 1). All data were log₂ transformed for subsequent analysis. Then, the POP1 expression was analyzed via the “ggplot” package in R software.

Mutation analysis and correlation analysis of clinical features

Mutation analysis was implemented in the cBioPortal database (<http://www.cbioportal.org>). Then, we selected the research cohort as “TCGA PanCancer Atlas Studies”, set the gene as “POP1”, and presented the mutation of POP1 in pan-cancer with a bar chart. Subsequently, we analyzed the association between POP1 and multiple clinical features. These analyses were performed in UALCAN database (<http://ualcan.path.uab.edu>). Select “TCGA” as the analysis object, “BC” as the tumor type, and “POP1” as the gene. The correlation between POP1

Table 1. Characteristics of included studies.

	Country	Platform	Normal	Mean0	SD0	Tumor	Mean1	SD1
TCGA	USA	NR	99	1.27	0.265	1072	1.84	0.61
GSE42568	Ireland	GPL570	17	3.11	0.859	104	3.61	0.674
GSE162228	China	GPL570	24	6.18	0.328	109	6.86	0.658
GSE7904	USA	GPL570	7	5.54	0.291	43	6.28	0.725
GSE161533	China	GPL570	28	4.49	0.184	28	4.74	0.379

and different clinical features, including stage and lymph node metastatic status, was subsequently obtained.

ROC curves of POP1 in different cohorts were established to assess the POP1 diagnostic accuracy

To evaluate the POP1 diagnostic value for BC, we established receiver operating characteristic (ROC) curves in 1 TCGA BC cohort and 4 GEO BC cohorts (GSE7904 cohort, GSE42568 cohort, GSE161533 cohort, GSE162228 cohort). ROC curves were built and the area under the curve (AUC) was counted via the “pROC” R package.

Meta-analysis of multiple cohorts to further verify the role of POP1 in BC

In order to exclude independent cohort bias, we included the 5 cohorts mentioned above including the TCGA cohort, GSE42568 cohort, GSE162228 cohort, GSE7904 cohort, and GSE161533 cohort to perform the meta-analysis to verify the expression of POP1 in BC. If the 95% confidence interval (CI) of the standardized mean difference (SMD) after the combination was greater than 0, the expression of POP1 was higher in BC. The test criteria for heterogeneity were as follows: if $I^2 > 50\%$, the random effect model was adopted; if $I^2 < 50\%$, the fixed-effect model was adopted. Subsequently, analysis of sensitivity and specificity were performed to verify the meta-analysis results' credibility. The accuracy of the meta-analysis was verified via establishing the summary receiver operating characteristic (SROC) curve and counting the AUC value. Egger test and Begg test were utilized to assess the publication bias size. The “meta” and “forest” packages in R software and the Stata software were applied to complete the above analysis.

Survival analysis of POP1 to explore its prognostic value

POP1 survival analysis was conducted on the TCGA cohort. According to the median POP1 expression, BC patients were divided into high- and low-POP1 groups. The prognosis difference between two groups was

analyzed by survival analysis which was performed via the “Survival” R package.

Gene Ontology (GO) enrichment analysis and Gene Set Enrichment Analysis (GSEA)

GO Enrichment analysis was carried out to explore the correlation of molecular functions and signaling pathways between POP1 and BC. The clusterProfile R package was utilized to analyze differential genes and their functional enrichment between the high- and low-POP1 group. Subsequently, GSEA was conducted to calculate the corresponding enrichment score for each known gene set.

Correlation analysis of POP1 and immune microenvironment

The differences in immune cell infiltration levels were investigated by the “CIBERSORT” database. The pheatmap R package was utilized to establish an immune landscape for BC. The “ggplot” R package was applied to establish a histogram of different immune cell infiltration. Subsequently, the Spearman correlation test was conducted to calculate the association between POP1 expression and distinct immune cells. Finally, the differential infiltration and high correlation of immune cell types were obtained via the Venn diagram, and the different infiltrated immune cell types were intersected with highly correlated immune cell types.

Construction of the POP1-related nomogram

Nomograms are diffusely used in cancer prognosis, mainly because they can reduce statistical prediction models to a single numerical estimate of an event probability, which can be customized to each patient's situation. To better assess the BC patients' prognosis, we established a nomogram according to the expression level and clinical correlation of POP1. The “Regplot” R package was utilized for the construction of the nomogram. The patient ID was: TCGA-E2-A14Z. We then constructed the 3-, 4-, and 5-year calibration curves of the nomogram to evaluate its accuracy.

Exploration of immune characteristics and prediction of immunotherapy response

According to the “estimate” R package (version 4.0.2), three scores were counted. The expression of 53 immune checkpoint-related genes was extracted to analyze for differential expression. We used Tumor Immune Dysfunction and Exclusion (TIDE) analysis to accurately simulate immune evasion and predict tumor immunotherapy response [28]. Patients with a TIDE score > 0 were considered unresponsive to immunotherapy, and patients with TIDE score < 0 were considered responsive to immunotherapy. In addition, a subclass mapping algorithm was performed to determine whether patients in high- and low-POP1 groups were suitable for immunotherapy [29]. Moreover, differential expression analysis of drug sensitivity (half maximal inhibitory concentration, IC50) was performed to identify suitable potential targeted drugs.

Cell transfection and real-time reverse transcription-PCR (qRT-PCR)

MDA-MB-231 and MCF-7 cells (American Type Culture Collection, Manassas, VA, USA) were cultured in Dulbecco's modified Eagle's medium (DMEM; Gibco, Carlsbad, CA, USA) added with 10% fetal bovine serum (FBS; Gibco, Carlsbad, CA, USA) at 37° C with 5% CO₂ atmosphere. All sequences of small interference RNA (siRNA; Ribobio, Guangzhou, China) for POP1 were available in Supplementary Table 1. The Lipofectamine 3000 Transfection Reagent (Invitrogen, Carlsbad, CA, USA) was utilized to transfect. After 24 h, qRT-PCR was utilized to assess transfection effectiveness. Total RNAs were isolated from cultivated BC cells and fresh clinical tissue samples using TRIzol (Takara, Japan). The 1st Strand cDNA Synthesis Kit (Yeasen, Shanghai, China) was utilized to generate cDNA. With SYBR Green™ Master Mix (Yeasen, Shanghai, China), the qRT-PCR was performed in QuantStudio1 (ABI Q1, USA). All qRT-PCR primer sequences were designed and launched by Tsingke (Beijing, China) and were available in Supplementary Table 2.

Cell viability and invasion assay

The CCK-8 method (Yeasen, Shanghai, China) was applied to assess the proliferative abilities of two cells. After seeding in 96-well plates, MDA-MB-231 and MCF-7 cells were cultured to 40% confluence at 37° C. 10 μL CCK-8 reagent was added after transfection. The optical density (OD) was detected at 450 nm at 0, 24, 48, and 72 h after CCK-8 reagent supplementation.

Cells were resuspended with 200 μL serum-free DMEM and implanted into 24 well transwell migration

chambers (8 μm pore size; Corning, NY, USA) inner chambers to conduct transwell migration assays. 700 μL DMEM medium containing 20% FBS, as an attractant, was injected into the bottom chambers. The chamber membranes were soaked in 4% paraformaldehyde for 30 min after incubation for 24 h, and cotton swabs were used to wipe the upper part of the chamber to eliminate non-migrated cells. Afterward migrated cells on the membrane lower side were stained with 0.1% crystal violet for 30 min at 37° C. The ImageJ software was applied for measuring the quantity of migrated cells.

The migration abilities of siRNA transfected cells were tested by wound healing assay. Transfected MDA-MB-231 and MCF-7 cells were seeded in the 6 well plates and grown to 90% confluent cell monolayer. With the 200 μL micropipette tip, the single-cell layer was scratched in each well. Then, the detached cells and debris were washed with phosphate-buffered saline (PBS), and the serum-free DMEM medium was added to each well. The 24 h horizontal distance of migrated cells was observed and measured using microscopy and ImageJ software.

Flow cytometry was applied to detect cell apoptosis with Annexin V-FITC/PI apoptosis kit (MultiSciences, Hangzhou, China). Cells were plated into 6-well plates and cultured for 24 h with siRNAs. Cells were collected, stained via Annexin V-FITC/PI for 5 min, and detected via flow cytometry.

Availability of data and materials

The datasets provided for this study can be found in online repositories. The name and accession number(s) of the repository/repositories can be found in the article Supplementary Materials.

RESULTS

POP1 expression in multiple BC cohorts

Firstly, in the TCGA BC cohort, POP1 expression was significantly higher in BC tissue than in normal breast tissue (Figure 1A). Subsequently, by using the GEO datasets, POP1 was overexpressed in BC tissues in the GSE7904 cohort, GSE42568 cohort, GSE161533 cohort, and GSE162228 cohort (Figure 1B–1E). Therefore, the POP1 was an up-regulated indicator in BC tissues from TCGA and GEO datasets.

Mutation analysis and correlation analysis of clinical features

First, mutation analysis of the TCGA pan-cancer cohort revealed that POP1 mutation frequency in BC

ranked fourth among all tumor types (Figure 2A). Subsequent analysis of the UALCAN database also suggested that the POP1 expression was higher in BC than in normal breast tissue (Figure 2B). Subgroup analysis demonstrated that POP1 was overexpressed in BC regardless of stage or lymph node metastasis status (Figure 2C, 2D).

ROC curves of POP1 in different cohorts were constructed to evaluate the diagnostic accuracy of POP1

To verify the diagnostic accuracy of POP1 for BC, we constructed ROC curves in multiple cohorts and calculated the corresponding AUC values. The AUC of POP1 in the TCGA cohort was 0.818 (Figure 3A). The AUC of POP1 was 0.844 (Figure 3B), 0.790 (Figure 3C), 0.718 (Figure 3D), and 0.849 (Figure 3E) in GSE7904 cohort, GSE42568 cohort, GSE161533 cohort, and GSE162228 cohort respectively. This demonstrated that POP1 had high accuracy in the diagnosis of BC.

Meta-analysis of multiple cohorts to demonstrate the POP1 role in BC

The above 5 cohorts (1 TCGA cohort, 4 GEO Cohorts) were jointly analyzed to exclude bias. The results

suggested that the heterogeneity was less than 50%, so the fixed effect model was applied for analysis (Figure 4A, SMD = 0.95, 95% CI: 0.78, 1.12). This indicated that POP1 was still highly expressed in the BC group after the combination. Subsequently, it found that regardless of the exclusion of any cohort, the combined SMD was greater than 0 (Figure 4B). In addition, sensitivity analysis and specificity analysis also showed the same results, indicating that the results of the meta-analysis were relatively robust (Figure 4C). SROC curve showed that the results were reliable (Figure 4D, AUC = 0.90, 95% CI: 0.87-0.92). Begg test and Egger test did not find significant publication bias (Figure 4E, 4F).

Analysis of POP1 survival and clinical correlation in BC

According to the POP1 median expression level, BC patients were divided equally into the high- and low-POP1 group in the TCGA cohort. The results of survival analysis suggested that the high-POP1 expression was correlated with the BC poor prognosis (Figure 5A). Univariate and multivariate Cox regression analysis showed that the high expression of POP1 was associated with low overall survival (OS) (Table 2, HR = 1.5, P = 0.012). This demonstrated that POP1 overexpression was independently related to low OS in BC patients.

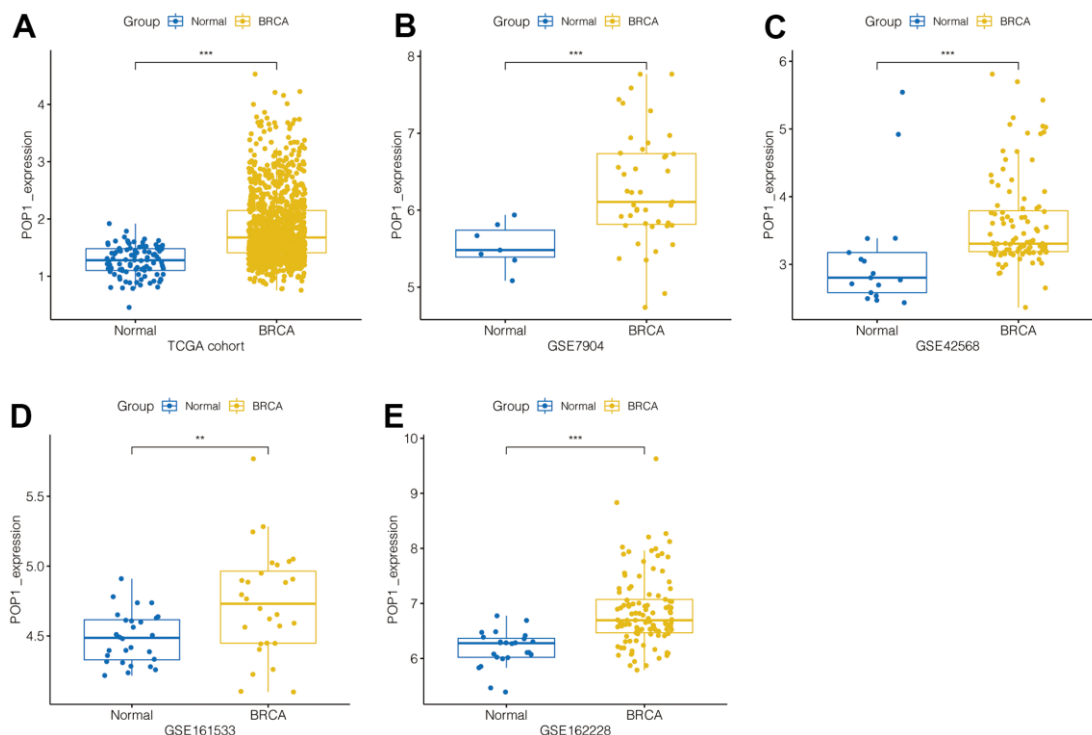


Figure 1. POP1 expression in BC. POP1 expression between non-BC tissues and BC tissues based on The Cancer Genome Atlas (TCGA) and Gene Expression Omnibus (GEO) datasets. (A) TCGA cohort. (B) GSE7904. (C) GSE42568. (D) GSE61533. (E) GSE162228. ** P < 0.01; *** P < 0.001. Abbreviations: TCGA, The Cancer Genome Atlas; GEO, Gene Expression Omnibus.

Analysis of clinical correlation suggested that POP1 expression was obviously related to age, T stage, and total stage (Figure 5B).

GSEA and GO enrichment analysis

To explore the carcinogenic mechanism of POP1 in BC, it was necessary to analyze the relationship between POP1 and corresponding functions and

signaling pathways. Firstly, GSEA analysis indicated that POP1 was significantly correlated with the E2F target, G2M checkpoint, interferon-gamma response, mitTORC1 signaling, and MYC targets (Figure 6A–6H). Subsequently, GO enrichment analysis verified that the differentially expressed genes were primarily interested in functional pathways, including organelle fission, nuclear division, and chromosome segregation (Figure 6I).

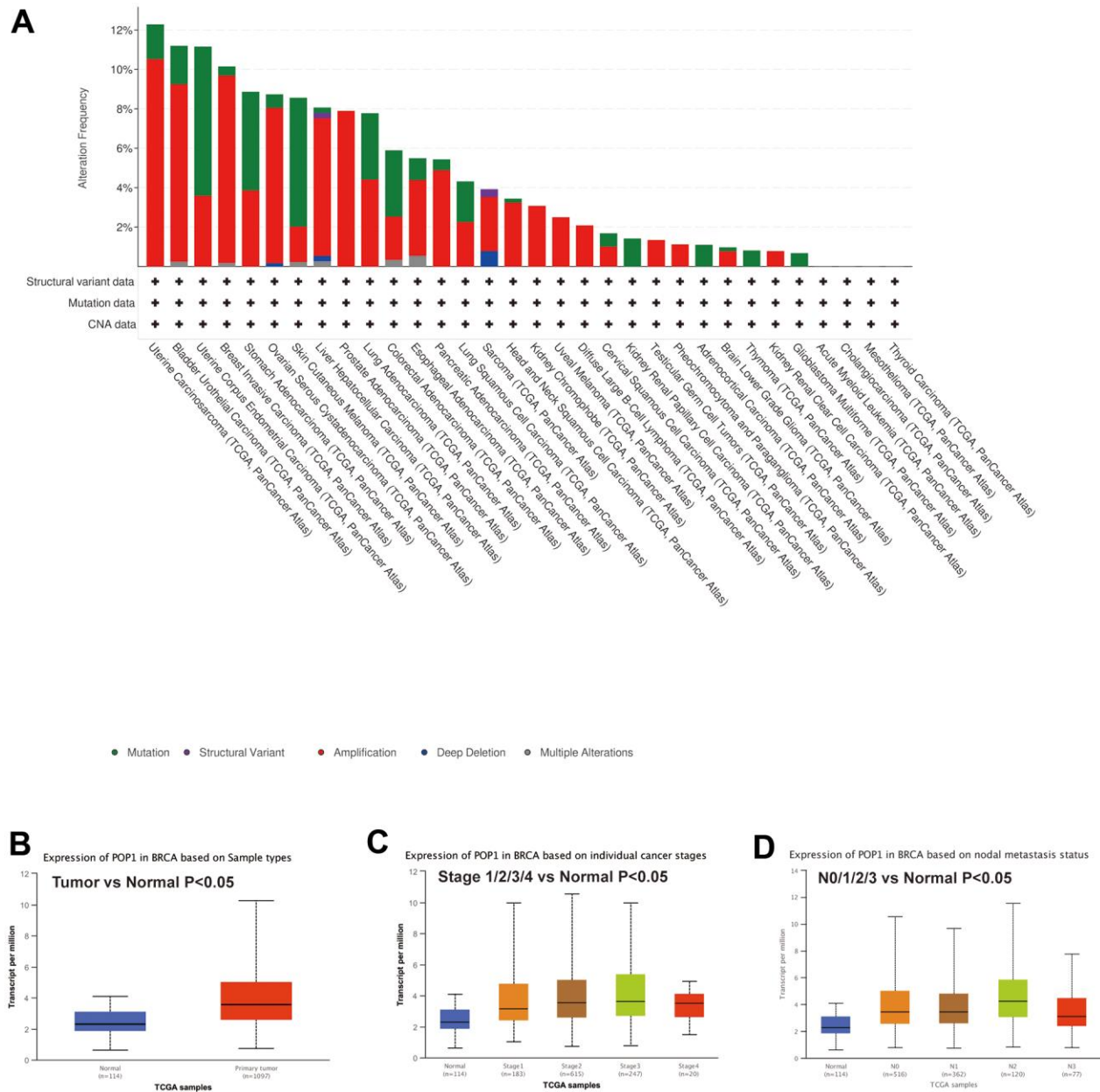


Figure 2. Mutation status of POP1 gene based on cBioPortal and the relationship between POP1 expression and clinical features of BC based on UALCAN databases. (A) Mutation analysis of the cBioPortal database showed that POP1 was the fourth most common mutation in BC. (B) UALCAN database also suggested that POP1 was more highly expressed in BC than in normal breast tissue. (C, D) Subgroup analysis verified that POP1 expression was higher in BC than in normal tissues regardless of stage or lymph node metastasis status.

Analysis of correlation between POP1 and immune microenvironment

Figure 7A showed the landscape of immune cell infiltration in BC. Through this heat map, the abundance of each immune cell was intuitively observed. Figure 7B presented different analysis results of immune cell infiltration in the two groups. T cells CD4 memory resting, T cells CD4 memory activated, Plasma cells, T cells regulatory (Tregs), T cells Follicular helper, natural killer (NK) cells resting, mast cells resting, macrophages M0, macrophages M1, macrophages M2, monocyte, dendritic cells (DCs) resting and DCs activated were differently infiltrated between the high- and low-POP1 group. Subsequent analysis of correlation verified that POP1 expression was related to many immune cells (Figure 7C–7M). Venn diagram intersected the differentially infiltrated immune cell types with highly correlated immune cell types, resulting in 10 immune cell types (Figure 7N).

Nomogram construction based on POP1 expression

Subsequently, we constructed a nomogram for POP1 by integrating POP1 expression and clinical data. The 1-, 3-,

and 5-year mortality forecasted by this nomogram was 0.0131, 0.0720, and 0.1300, respectively (Figure 8A). Based on the agreement between observed and predicted values, a nomogram calibration diagram of the training cohort was established. The 3-, 4-, and 5-year calibration curves verified the accuracy of the nomogram results (Figure 8B).

Analysis of immunity and immunotherapy response

Calculate 3 scores for all samples of BC according to the ESTIMATE algorithm. All three scores were found to differ significantly between the high- and low-POP1 groups (Figure 9A–9C). Considering the vital role of ICB therapy in the tumor, 53 checkpoint-relevant genes were screened for differential expression analysis in the samples. The expression of most immune checkpoints differed significantly in the two groups (Figure 9D). Meanwhile, the correlation between POP1 and the four most common immune checkpoints suggested that POP1 expression was positively related to the expressions of CTLA-4, PD-1, PD-L1, and PD-L2 (Figure 9E).

Based on the TIDE algorithm, we calculated the TIDE score, microsatellite instability (MSI) score, dysfunction

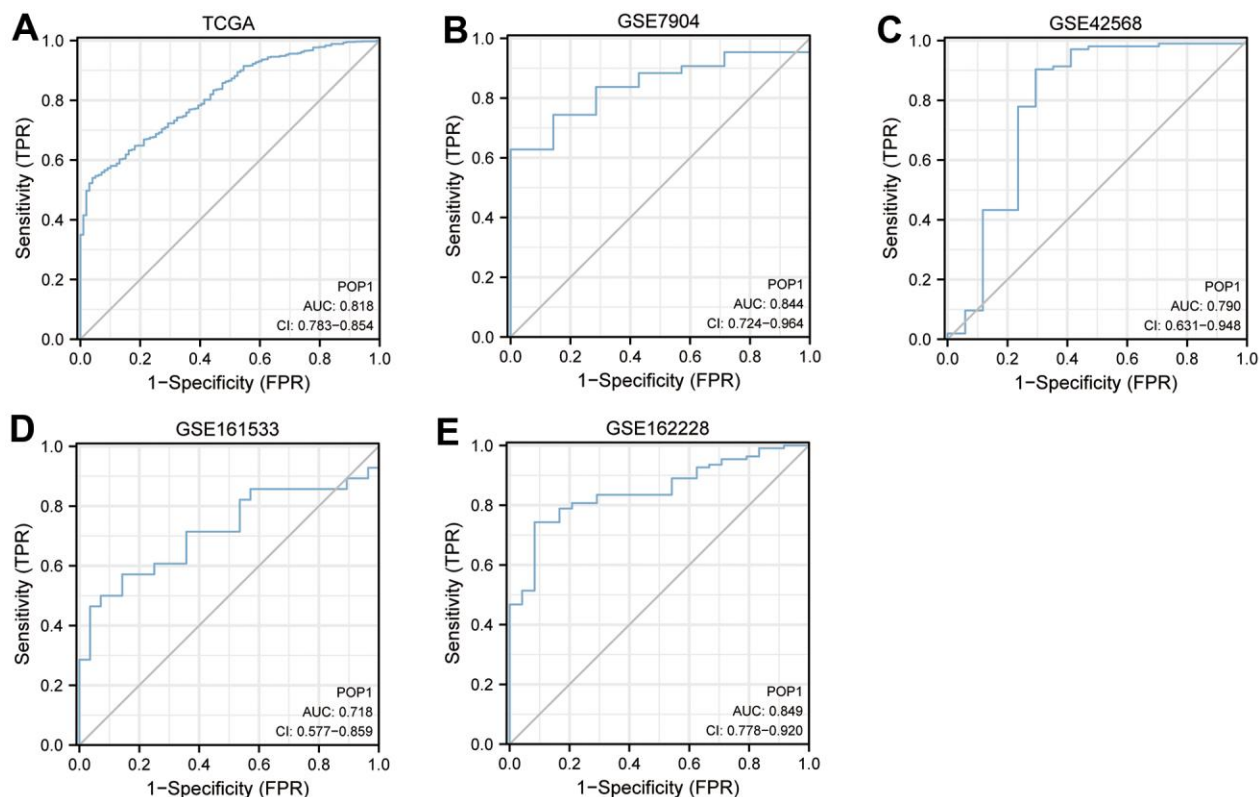


Figure 3. Diagnosis value of POP1. The receiver operating characteristic (ROC) curve to obtain the area under the curve (AUC) value of POP1 in different BC cohorts. (A) The Cancer Genome Atlas (TCGA) cohort. (B) GSE7904. (C) GSE42568. (D) GSE61533. (E) GSE162228. Abbreviations: ROC, Receiver operating characteristic; AUC, Area under the curve; TCGA, The Cancer Genome Atlas.

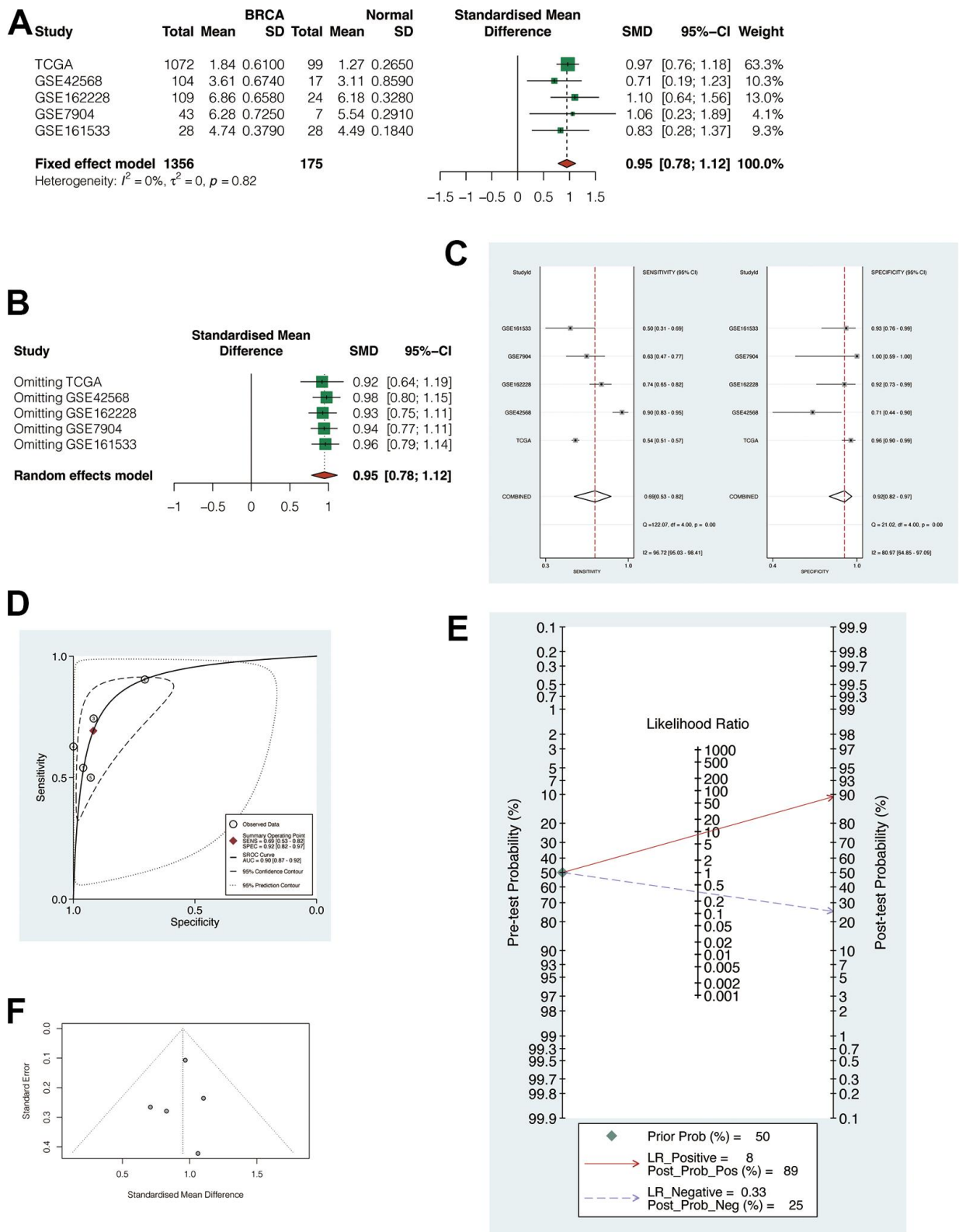


Figure 4. Meta-analysis of multiple cohorts to verify the robustness of POP1. (A) Meta-analysis. The heterogeneity was $< 50\%$, so the fixed effect model was used for analysis (SMD = 0.95, 95% CI: 0.78, 1.12). (B) Regardless of the exclusion of any cohort, the combined standardized mean difference (SMD) was greater than 0. (C) Sensitivity analysis and specificity analysis. (D) The summary receiver operating characteristic (SROC) curve demonstrated that the results are reliable. (E, F) Begg test and Egger test did not find significant publication bias. Abbreviations: SMD, Standardized mean difference; SROC, Summary receiver operating characteristic.

Table 2. Univariate and multivariate Cox analysis of breast cancer patients' overall survival.

Characteristics	Total(N)	Univariate analysis		Multivariate analysis	
		HR(95% CI)	P value	HR(95% CI)	P value
T stage	1079				
T1	276	Reference			
T2	629	1.334 (0.889-2.002)	0.164	0.770 (0.337-1.757)	0.534
T3	139	1.572 (0.933-2.649)	0.089	0.793 (0.296-2.122)	0.644
T4	35	3.755 (1.957-7.205)	<0.001	1.187 (0.354-3.985)	0.782
N stage	1063				
N0	514	Reference			
N1	357	1.956 (1.329-2.879)	<0.001	1.133 (0.575-2.234)	0.718
N2	116	2.519 (1.482-4.281)	<0.001	1.771 (0.531-5.912)	0.353
N3	76	4.188 (2.316-7.574)	<0.001	3.051 (1.011-9.208)	0.048
M stage	922				
M0	902	Reference			
M1	20	4.254 (2.468-7.334)	<0.001	6.989 (1.200-40.699)	0.031
Pathologic stage	1059				
Stage I	180	Reference			
Stage II	619	1.697 (0.985-2.922)	0.057	2.266 (0.694-7.397)	0.175
Stage III	242	2.962 (1.664-5.273)	<0.001	5.012 (1.024-24.517)	0.047
Stage IV	18	11.607 (5.569-24.190)	<0.001		
Age	1082				
<=60	601	Reference			
>60	481	2.020 (1.465-2.784)	<0.001	2.393 (1.495-3.831)	<0.001
Race	993				
Asian	60	Reference			
Black or African American	180	1.525 (0.463-5.024)	0.488		
White	753	1.325 (0.420-4.186)	0.631		
Histological type	977				
Infiltrating Ductal Carcinoma	772	Reference			
Infiltrating Lobular Carcinoma	205	0.827 (0.526-1.299)	0.410		
PR status	1033				
Negative	342	Reference			
Indeterminate	4	0.826 (0.113-6.035)	0.851		
Positive	687	0.732 (0.524-1.025)	0.069		
ER status	1034				
Negative	240	Reference			
Indeterminate	2	13.088 (3.128-54.771)	<0.001		
Positive	792	0.712 (0.495-1.023)	0.066	0.467 (0.276-0.790)	0.005
HER2 status	727				
Negative	558	Reference			
Indeterminate	12	0.000 (0.000-Inf)	0.994		
Positive	157	1.593 (0.973-2.609)	0.064		
Radiation therapy	986				
No	434	Reference			
Yes	552	0.576 (0.394-0.841)	0.004	0.434 (0.267-0.704)	<0.001
POP1	1082				
Low	540	Reference			
High	542	1.538 (1.110-2.130)	0.010	1.706 (1.021-2.850)	0.041

Furthermore, we analyzed the immune cells and correlative immune pathways in two risk groups. Patients with high-risk scores got a higher level of most immune signatures. CTLA-4, PD-1, PD-L1, and PD-L2 levels were higher in high-risk patients. PD-L1 expression has been demonstrated as a potential target for cancer immunotherapy [33]. Meanwhile, PD-1 expression increases neuronal killing of tumor cells and is linked to prolonged survival [34]. TIDE analysis revealed that the immunotherapy response rate in the high-risk group was higher than that in the low-risk group, which might be related to the level of immune-checkpoint-relevant genes. The results of subclass mapping algorithm analysis verify our findings that PD-1 checkpoint therapy was more likely to be effective in the high-POP1 group. Finally, by verifying the effect of POP1 *in vitro*, it was confirmed that POP1 promoted the viability and invasion of BC

cells. These results were consistent with the previous results.

Malignant tumors often lack accurate prognostic markers. In the past, some biomarkers, such as PD-1, LAG-3, EGFR, and CD44, are found to have prognostic or therapeutic value in BC [35]. However, BC is a heterogeneous group, and these existing biomarkers are not sufficient to meet the needs [36]. It is urgent to explore new and robust targets to guide diagnosis and treatment. Our study found that POP1 expression was up-regulated in multiple BC cohorts and was linked to poor prognosis. All of these indicated that POP1 was a robust prognostic marker of BC.

GO enrichment analysis verified that the POP1 overexpression in BC was closely related to the

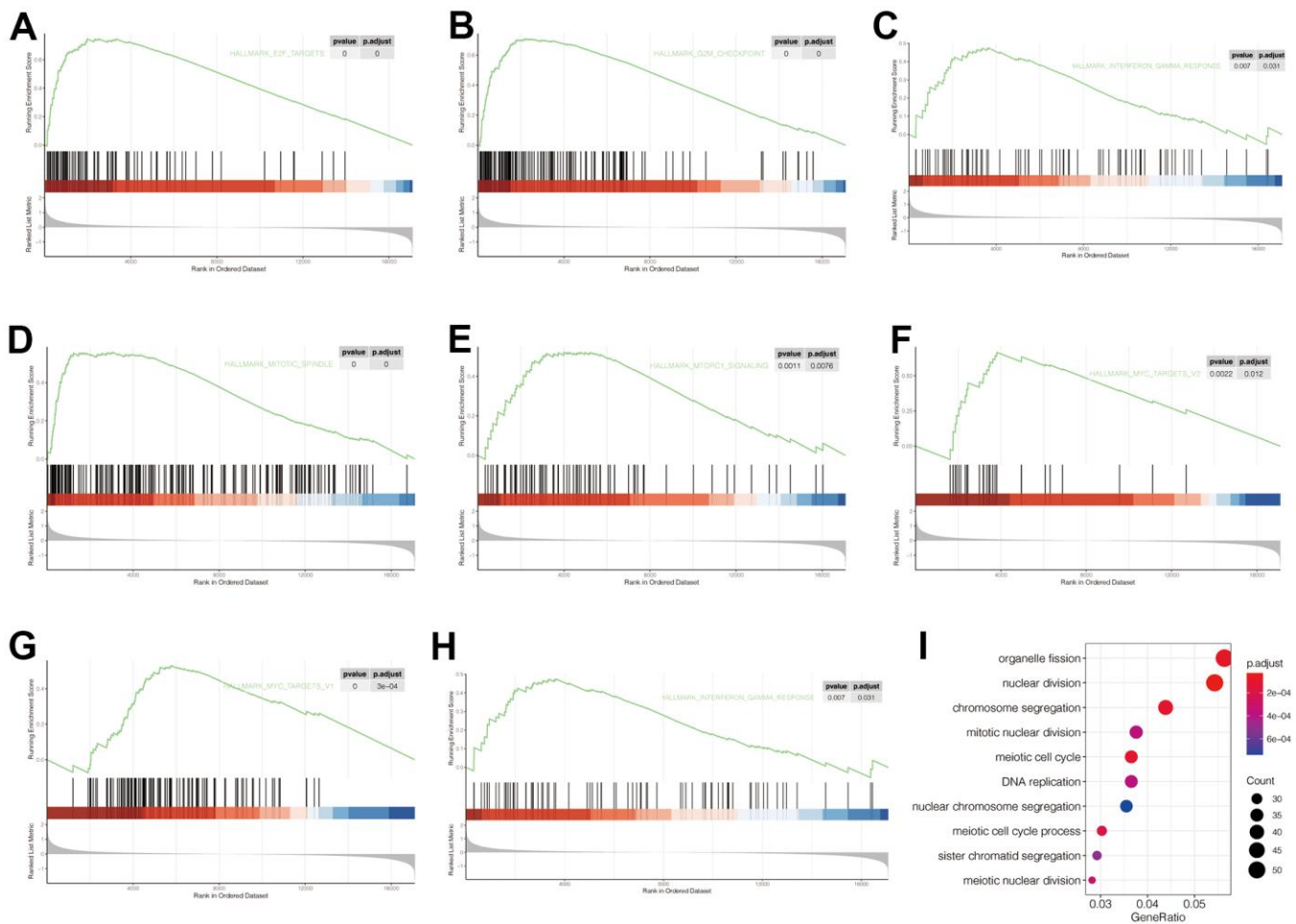


Figure 6. Gene Set Enrichment Analysis (GSEA) and Gene Ontology (GO) of corresponding functions and signaling pathways associated with POP1 expression. (A–H) The POP1 expression was significantly correlated with the E2F target, G2M checkpoint, interferon-gamma response, mitTORC1 signaling, and MYC targets. **(I)** The differentially expressed genes between the high- and low-POP1 groups were mainly enriched in organelle fission, nuclear division, and chromosome segregation. Abbreviations: GSEA, Gene set enrichment analysis; GO, Gene Ontology.

activation of cell proliferation-related pathways. Cell cycle disorder is one of the characteristics of cancer, which can result in unbounded cell proliferation and cancer development [37, 38]. The disorder of cell proliferation and metastasis is an important reason for

the occurrence and development of tumors [39]. Overall, the GSEA analysis demonstrated the preceding speculation that the POP1 overexpression appeared to be more likely associated with the enhancement of BC cell growth and metastasis. In addition, POP1 might

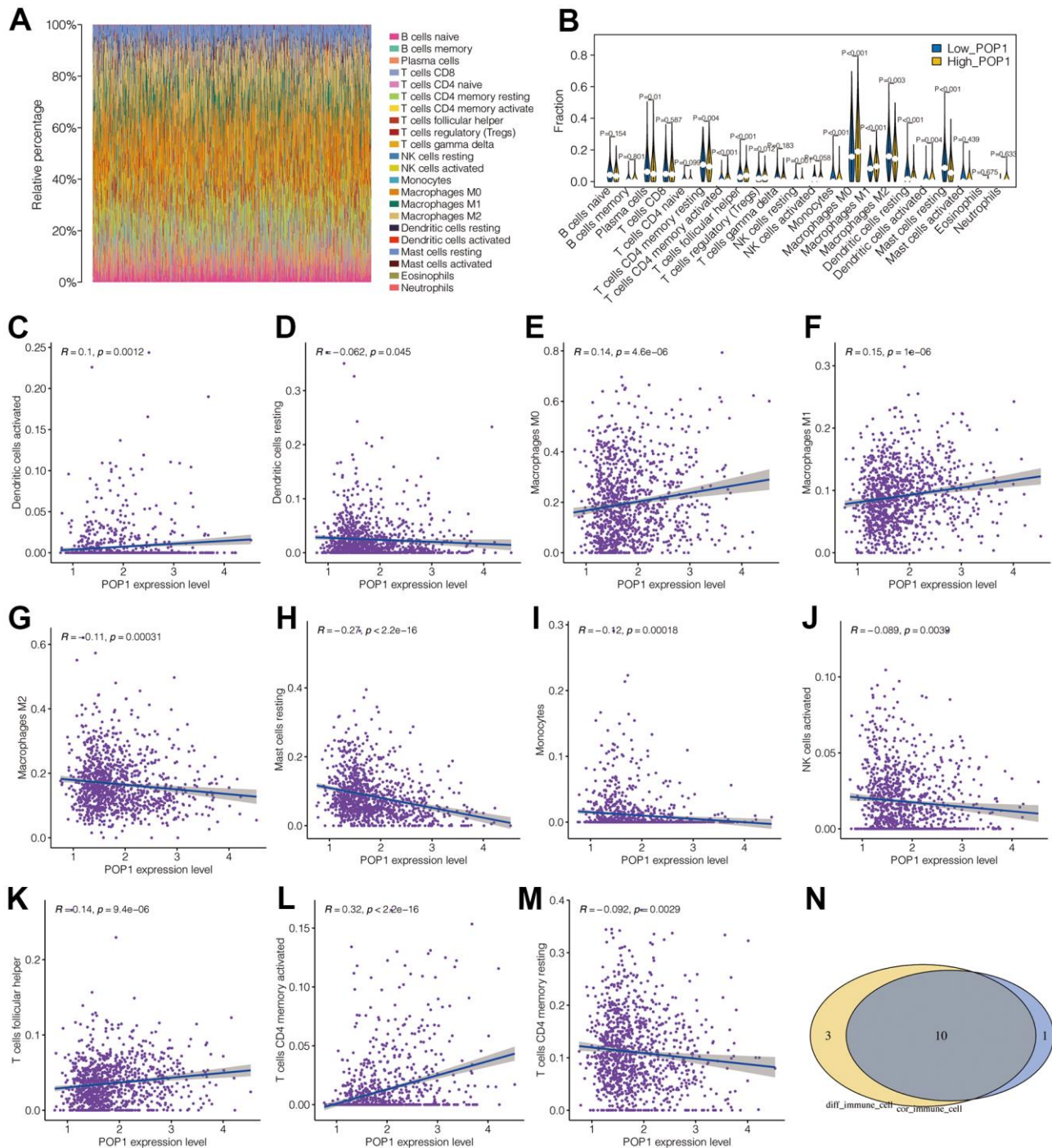


Figure 7. Correlation analysis between POP1 and immune microenvironment. (A) The landscape of immune cell infiltration in BC. (B) Difference analysis results of immune cell infiltration between the high- and low-POP1 group. (C–M) Correlation analysis showed that POP1 expression was correlated with a variety of immune cells. (N) A Venn diagram intersects the immune-cell types infiltrated differently with those associated with POP1.

play an important role by regulating crucial pathways, including organelle fission, nuclear division, and chromosome segregation pathways.

The BC immune microenvironment is quite complicated and heterogeneous [40]. The TME consists of the extracellular matrix, fibroblasts, cancer cells, immune cells, cytokines, chemokines, etc. However, immune cells and stromal cells, represent the primary non-tumor components of TME [41, 42]. Studies on TME verify that Effector T cell activation and the decrease in DC infiltration are two primary methods to decrease the

immune response to cancer therapy [43, 44]. However, the factors that regulate the TME components and affect the immune response to treatment remain to be investigated. Thus, it is essential to understand the correlation between the prognosis and TME for exploring effective immunotherapies. The relationship between TME and immunotherapy has attracted increasing attention lately. The response to immunotherapy depends on the number of immune cells infiltrating the tumor [45, 46]. Therefore, after identifying the prognostic value of POP1 in BC, it is necessary to analyze its role in the immune microenvironment of BC. Our study not

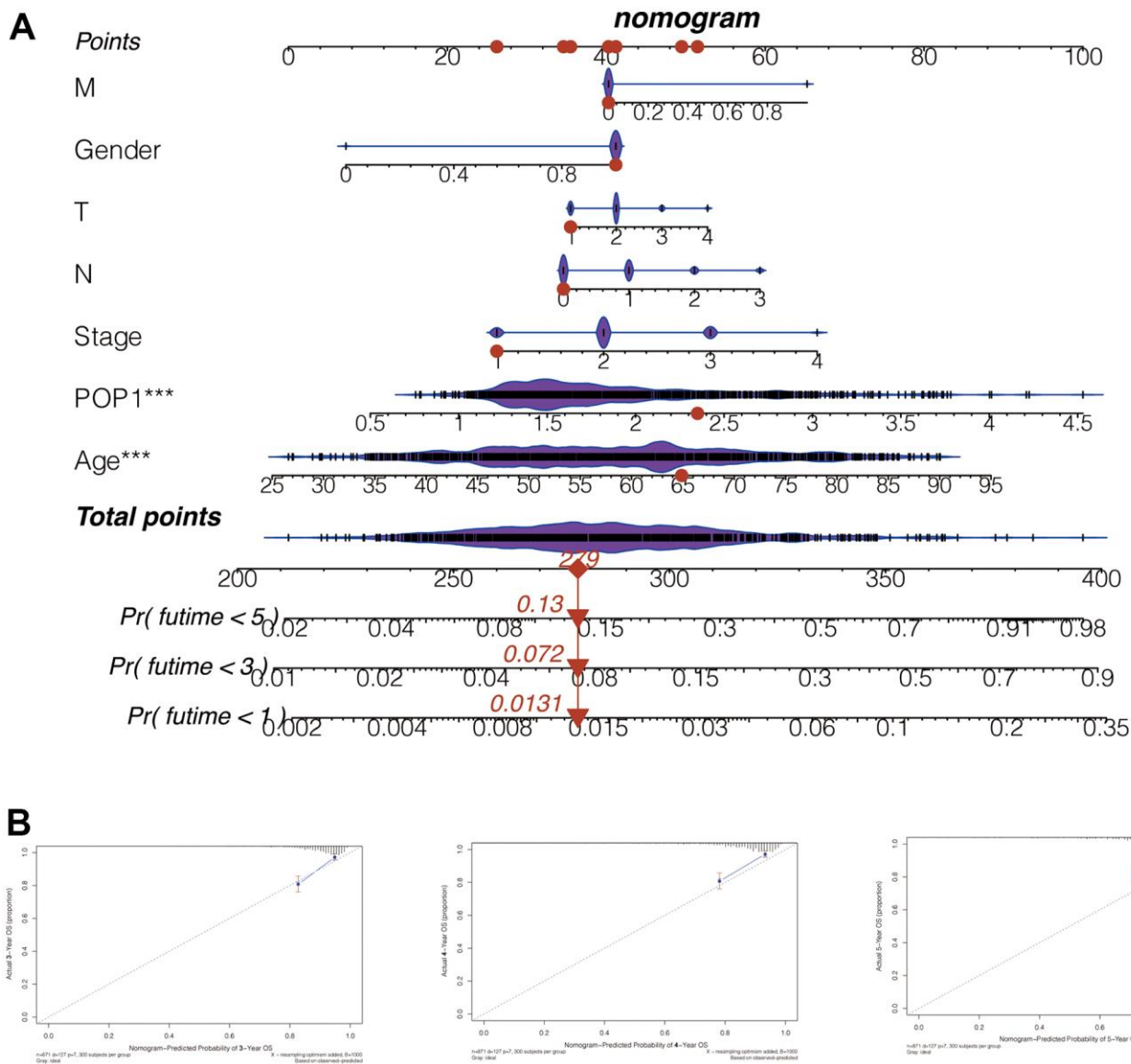


Figure 8. Nomogram to evaluate patient mortality. (A) The 1-, 3-, and 5-year mortality of BC patients predicted by this nomogram was 0.0131, 0.072, and 0.13, respectively. (B) According to the consistency between the observed and predicted values, the nomogram calibration plot of the training cohort was established. The calibration curves of 3, 4, and 5 years indicated that nomogram results are accurate.

only provides an immune landscape for BC but also identifies immune cells highly associated with POP1, which has a certain reference value for immunotherapy of BC.

Immunotherapy is a promising cancer treatment strategy with significant survival benefits for some BC patients. Tumor ICBs have been proven to be an effective treatment for many malignancies. However, BC is a highly heterogeneous tumor that renders immunotherapy ineffective for many patients [47]. ICBs are approved for the therapy of particular cancer types and have been involved in miscellaneous clinical trials, however, only a few patients have favorable responses [48]. ICB

antibodies targeting PD-1 or PD-L1 have the potential to treat metastatic BC, and the identification of BC patients who are responsive to immunotherapy is significant. Pembrolizumab, an anti-PD-1 antibody, has been found to enhance progression-free survival and OS in combination with chemotherapy for metastatic TNBC expressing PD-L1 [49]. However, in PD-L1-negative tumors, hormone-sensitive tumors, and pretreated advanced illnesses, the anti-PD-1/PD-L1 drug therapeutic is less noteworthy.

CTLA-4 is a surrogate target for immune checkpoint inhibition. Anti-CTLA-4 antibodies, including ipilimumab and tremelimumab, can improve the prognosis of

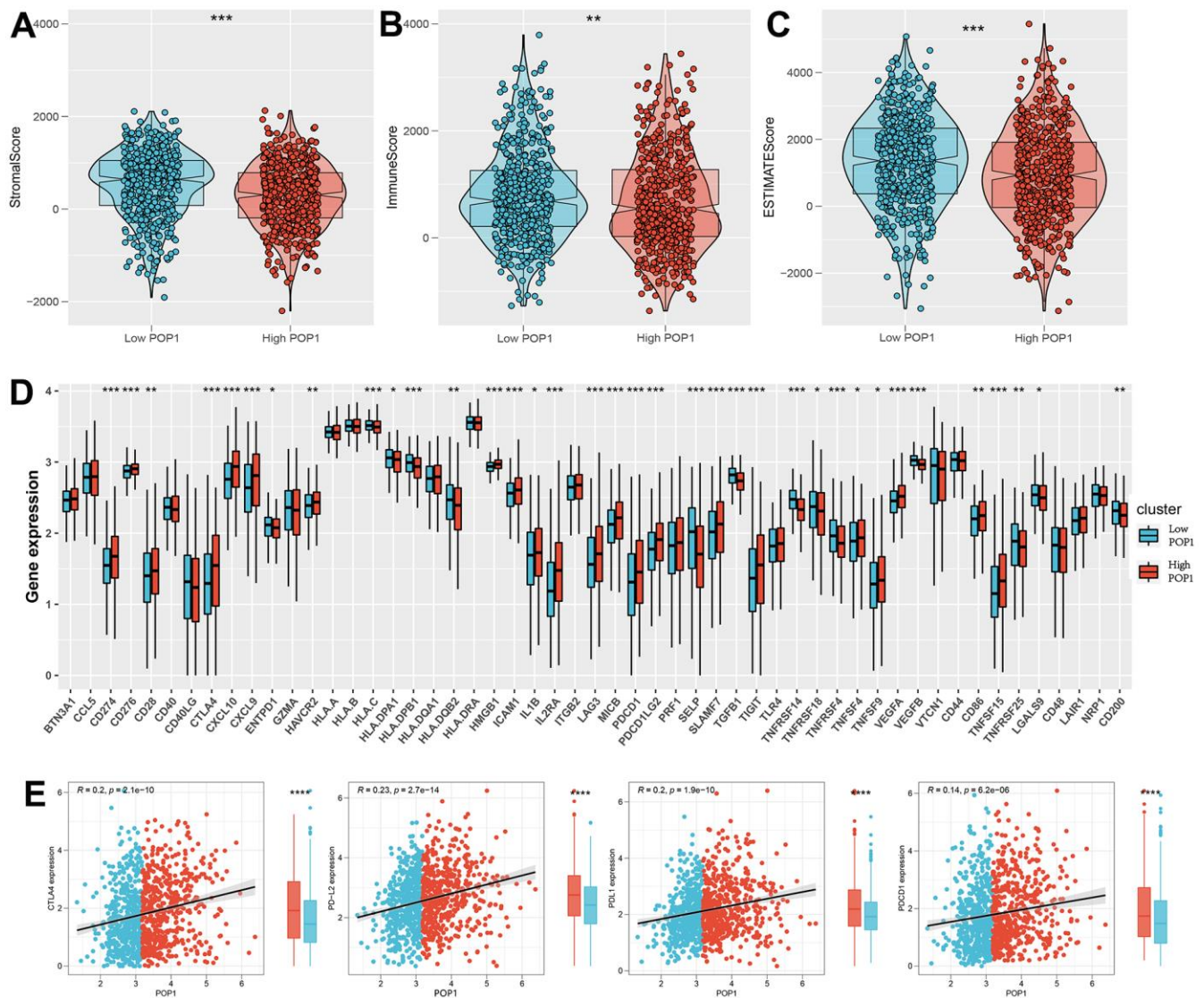


Figure 9. Investigate the differences in immune characteristics between the high- and low-POP1 groups. (A–C) Discrepancies in three scores between the high- and low-POP1 groups. **(D)** Expression differences of 53 immune characteristics between the high- and low-POP1 groups of BC patients. **(E)** Correlation analysis of four immune checkpoints in high- and low-POP1 population of BC patients. *P < 0.05; **P < 0.01; ***P < 0.001.

metastatic melanoma and boost anti-tumor responses in BC [50]. After T-cell antigen exposure and activation, CTLA-4 is rapidly up-regulated, while PD-1 is up-regulated and persists during chronic T-cell stimulation.

Anti-CTLA-4 and anti-PD-1/PD-L1 could react differently in distinct disease subtypes and clinical settings because of differences in these mechanistic. The latest research has emphasized novel combined methods that integrate

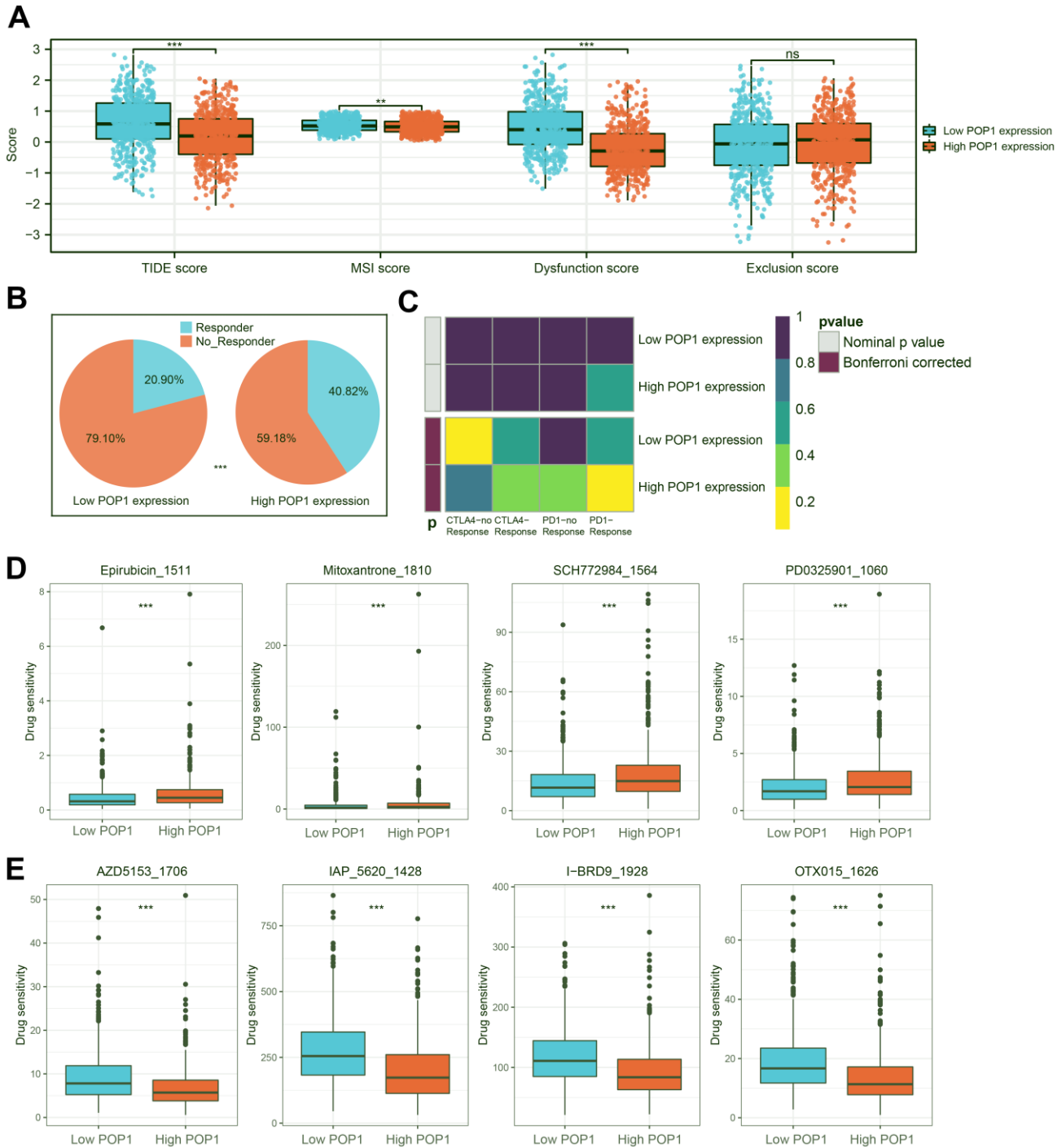


Figure 10. Immunotherapy response prediction and potential drug screening. (A) Distribution of Tumor Immune Dysfunction and Exclusion (TIDE) score, microsatellite instability (MSI) score, Dysfunction score, and Exclusion score. (B) Responder rates differed between the high- and low-POP1 groups. (C) A subclass mapping algorithm was used to verify the immunotherapy prediction results. (D, E) The drugs with the most significant difference in sensitivity between the high- and low-POP1 groups. ** $P < 0.01$; *** $P < 0.001$. Abbreviations: TIDE, Tumor Immune Dysfunction, and Exclusion; MSI, Microsatellite instability.

anti-CTLA-4 with other ICBs or traditional treatments to greatly enhance the efficacy of immunotherapy in many cancer types [51].

According to 5 datasets from the TCGA and GEO databases, the POP1 overexpression in BC and its

hopeful diagnostic and prognostic value were identified. Furthermore, we first explored the association between POP1 expression, immune properties, and immunotherapy response in BC patients. However, the limitations of this study still need to be addressed. We lack a BC cohort from our center to verify the

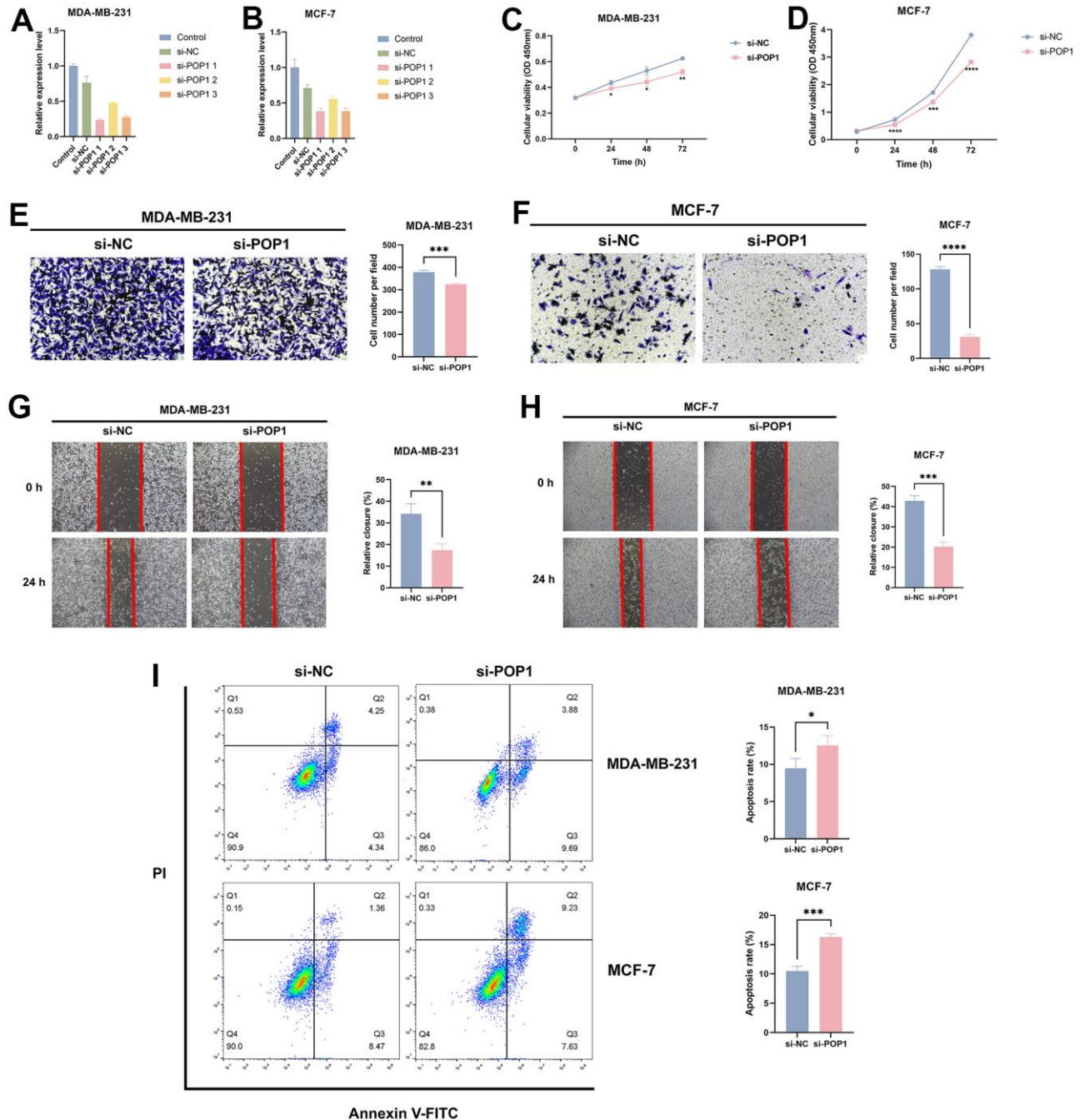


Figure 11. The effect of POP1 on proliferation, migration, and apoptosis of BC cells. (A, B) The qRT-PCR results suggested that siRNAs could successfully knock down the expression of POP1 in MDA-MB-231 and MCF-7. (C, D) Compared with the si-NC group, POP1 deficiency significantly inhibited the proliferation of MDA-MB-231 and MCF-7. (E–H) The depletion of POP1 significantly reduced the migration ability of MDA-MB-231 and MCF-7 cells, as demonstrated by transwell migration assays (magnification, 200×) and wound healing assays (magnification, 20×). (I) Cell apoptosis was detected via flow cytometry. *P < 0.05; **P < 0.01; ***P < 0.001, ****P < 0.0001.

prognostic value of POP1, needing to improve in the future. Moreover, our study is restricted to *in vitro* studies. In the future, more *in vitro*, especially *in vivo* studies are still needed to demonstrate the conclusions and investigate the concrete mechanism of POP1 in BC occurrence and development.

CONCLUSIONS

Overall, POP1 is a hopeful diagnostic and prognostic target for BC. POP1 is positively related to the expression of the four most common immune checkpoints: CTLA-4, PD-1, PD-L1, and PD-L2. Patients with high-POP1 expression may be sensitive to PD-1 therapy, while patients with low-POP1 expression may not be sensitive to CTLA-4 therapy.

Abbreviations

BC: Breast cancer; TCGA: The Cancer Genome Atlas; GEO: Gene Expression Omnibus; ER: Estrogen receptor; TNBC: Triple-negative breast cancer; ROC: Receiver operating characteristic; AUC: Area under the curve; CI: Confidence interval; SMD: Standardized mean difference; SROC: Summary receiver operating characteristic; GO: Gene Ontology; GSEA: Gene set enrichment analysis; siRNA: Small interference RNA; qRT-PCR: Real-time reverse transcription-PCR; OD: Optional density; DMEM: Dulbecco's modified Eagle's medium; FBS: Fetal bovine serum; PBS: Phosphate-buffered saline; Tregs: T cells regulatory; NK: Natural killer; DC: Dendritic cell; CCK-8: Cell Counting Kit-8; OS: Overall survival; CAR: Chimeric antigen receptor; ICB: Immune checkpoint blockade; PD-1: Programmed cell death protein-1; PD-L1: Programmed death ligand-1; CTLA-4: Cytotoxic T-lymphocyte-associated protein 4; TIDE: Tumor Immune Dysfunction and Exclusion; TIL: Tumor-infiltrating lymphocyte; TME: Tumor microenvironment; TIDE: Tumor Immune Dysfunction and Exclusion; MSI: Microsatellite instability.

AUTHOR CONTRIBUTIONS

QZ, ZL, and YW conceived the project. XH and JW analyzed the data. XH and HY conducted the experiments. Both XH and JW wrote and revised the article. WL and YW performed the literature investigation and revised the article, including figures and tables. All authors have reviewed the article and all approved the final version.

ACKNOWLEDGMENTS

We acknowledge TCGA and GEO databases for providing platforms and contributors for uploading meaningful datasets.

CONFLICTS OF INTEREST

The authors declare no conflicts of interest.

FUNDING

This work was supported by China GuangHua Science and Technology Foundation (grant number 2019JZXM001) and Wuhan Science and Technology Bureau (grant number 2020020601012241).

REFERENCES

1. Xie J, Wang M, Cao Y, Zhu Z, Ruan S, Ou M, Yu P, Shi J. ADM-assisted prepectoral breast reconstruction is not associated with high complication rate as before: a Meta-analysis. *J Plast Surg Hand Surg*. 2021; 1. <https://doi.org/10.1080/2000656X.2021.1981351> PMID:[34581645](https://pubmed.ncbi.nlm.nih.gov/34581645/)
2. Kolak A, Kamińska M, Sygit K, Budny A, Surdyka D, Kukiełka-Budny B, Burdan F. Primary and secondary prevention of breast cancer. *Ann Agric Environ Med*. 2017; 24:549–53. <https://doi.org/10.26444/aaem/75943> PMID:[29284222](https://pubmed.ncbi.nlm.nih.gov/29284222/)
3. Menta A, Fouad TM, Lucci A, Le-Petross H, Stauder MC, Woodward WA, Ueno NT, Lim B. Inflammatory Breast Cancer: What to Know About This Unique, Aggressive Breast Cancer. *Surg Clin North Am*. 2018; 98:787–800. <https://doi.org/10.1016/j.suc.2018.03.009> PMID:[30005774](https://pubmed.ncbi.nlm.nih.gov/30005774/)
4. Woolston C. Breast cancer. *Nature*. 2015; 527:S101. <https://doi.org/10.1038/527S101a> PMID:[26580154](https://pubmed.ncbi.nlm.nih.gov/26580154/)
5. Anastasiadi Z, Lianos GD, Ignatiadou E, Harissis HV, Mitsis M. Breast cancer in young women: an overview. *Updates Surg*. 2017; 69:313–7. <https://doi.org/10.1007/s13304-017-0424-1> PMID:[28260181](https://pubmed.ncbi.nlm.nih.gov/28260181/)
6. Veronesi U, Boyle P, Goldhirsch A, Orecchia R, Viale G. Breast cancer. *Lancet*. 2005; 365:1727–41. [https://doi.org/10.1016/S0140-6736\(05\)66546-4](https://doi.org/10.1016/S0140-6736(05)66546-4) PMID:[15894099](https://pubmed.ncbi.nlm.nih.gov/15894099/)
7. Hughes KS, Schnaper LA, Bellon JR, Cirincione CT, Berry DA, McCormick B, Muss HB, Smith BL, Hudis CA, Winer EP, Wood WC. Lumpectomy plus tamoxifen with or without irradiation in women age 70 years or older with early breast cancer: long-term follow-up of CALGB 9343. *J Clin Oncol*. 2013; 31:2382–7. <https://doi.org/10.1200/JCO.2012.45.2615> PMID:[23690420](https://pubmed.ncbi.nlm.nih.gov/23690420/)
8. Evron E, Ben-David AM, Goldberg H, Fried G, Kaufman B, Catane R, Pfeffer MR, Geffen DB, Chernobelsky P, Karni T, Abdah-Bortnyak R, Rosengarten O,

- Matceyevsky D, et al. Prophylactic irradiation to the contralateral breast for BRCA mutation carriers with early-stage breast cancer. *Ann Oncol*. 2019; 30:412–7. <https://doi.org/10.1093/annonc/mdy515> PMID:30475942
9. Ganz PA, Goodwin PJ. Breast Cancer Survivorship: Where Are We Today? *Adv Exp Med Biol*. 2015; 862:1–8. https://doi.org/10.1007/978-3-319-16366-6_1 PMID:26059925
 10. Maharana J, Vats A, Gautam S, Nayak BP, Kumar S, Sendha J, De S. POP1 might be recruiting its type-Ia interface for NLRP3-mediated PYD-PYD interaction: Insights from MD simulation. *J Mol Recognit*. 2017; 30. <https://doi.org/10.1002/jmr.2632> PMID:28370480
 11. Andrée B, Fleige A, Arnold HH, Brand T. Mouse Pop1 is required for muscle regeneration in adult skeletal muscle. *Mol Cell Biol*. 2002; 22:1504–12. <https://doi.org/10.1128/MCB.22.5.1504-1512.2002> PMID:11839816
 12. Srimathi T, Robbins SL, Dubas RL, Chang H, Cheng H, Roder H, Park YC. Mapping of POP1-binding site on pyrin domain of ASC. *J Biol Chem*. 2008; 283:15390–8. <https://doi.org/10.1074/jbc.M801589200> PMID:18362139
 13. Zhu D, Chen J, Hou T. Development and Validation of a Prognostic Model of RNA-Binding Proteins in Colon Adenocarcinoma: A Study Based on TCGA and GEO Databases. *Cancer Manag Res*. 2021; 13:7709–22. <https://doi.org/10.2147/CMAR.S330434> PMID:34675667
 14. Liang C, Fan J, Liang C, Guo J. Identification and Validation of a Pyroptosis-Related Prognostic Model for Gastric Cancer. *Front Genet*. 2022; 12:699503. <https://doi.org/10.3389/fgene.2021.699503> PMID:35280928
 15. Chen DS, Mellman I. Elements of cancer immunity and the cancer-immune set point. *Nature*. 2017; 541:321–30. <https://doi.org/10.1038/nature21349> PMID:28102259
 16. McGrail DJ, Pilié PG, Rashid NU, Voorwerk L, Slagter M, Kok M, Jonasch E, Khasraw M, Heimberger AB, Lim B, Ueno NT, Litton JK, Ferrarotto R, et al. High tumor mutation burden fails to predict immune checkpoint blockade response across all cancer types. *Ann Oncol*. 2021; 32:661–72. <https://doi.org/10.1016/j.annonc.2021.02.006> PMID:33736924
 17. Labanieh L, Majzner RG, Klysz D, Sotillo E, Fisher CJ, Vilches-Moure JG, Pacheco KZB, Malipatlolla M, Xu P, Hui JH, Murty T, Theruvath J, Mehta N, et al. Enhanced safety and efficacy of protease-regulated CAR-T cell receptors. *Cell*. 2022; 185:1745–63.e22. <https://doi.org/10.1016/j.cell.2022.03.041> PMID:35483375
 18. Ribas A, Wolchok JD. Cancer immunotherapy using checkpoint blockade. *Science*. 2018; 359:1350–5. <https://doi.org/10.1126/science.aar4060> PMID:29567705
 19. Garon EB, Rizvi NA, Hui R, Leighl N, Balmanoukian AS, Eder JP, Patnaik A, Aggarwal C, Gubens M, Horn L, Carcereny E, Ahn MJ, Felip E, et al, and KEYNOTE-001 Investigators. Pembrolizumab for the treatment of non-small-cell lung cancer. *N Engl J Med*. 2015; 372:2018–28. <https://doi.org/10.1056/NEJMoa1501824> PMID:25891174
 20. Chen L, Han X. Anti-PD-1/PD-L1 therapy of human cancer: past, present, and future. *J Clin Invest*. 2015; 125:3384–91. <https://doi.org/10.1172/JCI80011> PMID:26325035
 21. Dong H, Strome SE, Salomao DR, Tamura H, Hirano F, Flies DB, Roche PC, Lu J, Zhu G, Tamada K, Lennon VA, Celis E, Chen L. Tumor-associated B7-H1 promotes T-cell apoptosis: a potential mechanism of immune evasion. *Nat Med*. 2002; 8:793–800. <https://doi.org/10.1038/nm730> PMID:12091876
 22. Grosser R, Cherkassky L, Chintala N, Adusumilli PS. Combination Immunotherapy with CAR T Cells and Checkpoint Blockade for the Treatment of Solid Tumors. *Cancer Cell*. 2019; 36:471–82. <https://doi.org/10.1016/j.ccell.2019.09.006> PMID:31715131
 23. Cherkassky L, Morello A, Villena-Vargas J, Feng Y, Dimitrov DS, Jones DR, Sadelain M, Adusumilli PS. Human CAR T cells with cell-intrinsic PD-1 checkpoint blockade resist tumor-mediated inhibition. *J Clin Invest*. 2016; 126:3130–44. <https://doi.org/10.1172/JCI83092> PMID:27454297
 24. Hirsch L, Zitvogel L, Eggermont A, Marabelle A. PD-Loma: a cancer entity with a shared sensitivity to the PD-1/PD-L1 pathway blockade. *Br J Cancer*. 2019; 120:3–5. <https://doi.org/10.1038/s41416-018-0294-4> PMID:30413824
 25. Bahwal SA, Chen JJ, E L, Hao T, Chen J, Carruthers VB, Lai J, Zhou X. Attenuated *Toxoplasma gondii* enhances the antitumor efficacy of anti-PD1 antibody by altering the tumor microenvironment in a pancreatic cancer mouse model. *J Cancer Res Clin Oncol*. 2022. [Epub ahead of print]. <https://doi.org/10.1007/s00432-022-04036-8> PMID:35556163

26. Rosenberg JE, Hoffman-Censits J, Powles T, van der Heijden MS, Balar AV, Necchi A, Dawson N, O'Donnell PH, Balmanoukian A, Loriot Y, Srinivas S, Retz MM, Grivas P, et al. Atezolizumab in patients with locally advanced and metastatic urothelial carcinoma who have progressed following treatment with platinum-based chemotherapy: a single-arm, multicentre, phase 2 trial. *Lancet*. 2016; 387:1909–20.
[https://doi.org/10.1016/S0140-6736\(16\)00561-4](https://doi.org/10.1016/S0140-6736(16)00561-4)
PMID:[26952546](https://pubmed.ncbi.nlm.nih.gov/26952546/)
27. Xie J, Chen L, Cao Y, Wu D, Xiong W, Zhang K, Shi J, Wang M. Single-Cell Sequencing Analysis and Weighted Co-Expression Network Analysis Based on Public Databases Identified That TNC Is a Novel Biomarker for Keloid. *Front Immunol*. 2021; 12:783907.
<https://doi.org/10.3389/fimmu.2021.783907>
PMID:[35003102](https://pubmed.ncbi.nlm.nih.gov/35003102/)
28. Jiang P, Gu S, Pan D, Fu J, Sahu A, Hu X, Li Z, Traugh N, Bu X, Li B, Liu J, Freeman GJ, Brown MA, et al. Signatures of T cell dysfunction and exclusion predict cancer immunotherapy response. *Nat Med*. 2018; 24:1550–8.
<https://doi.org/10.1038/s41591-018-0136-1>
PMID:[30127393](https://pubmed.ncbi.nlm.nih.gov/30127393/)
29. Hoshida Y, Brunet JP, Tamayo P, Golub TR, Mesirov JP. Subclass mapping: identifying common subtypes in independent disease data sets. *PLoS One*. 2007; 2:e1195.
<https://doi.org/10.1371/journal.pone.0001195>
PMID:[18030330](https://pubmed.ncbi.nlm.nih.gov/18030330/)
30. Sun J, Li B, Shu C, Ma Q, Wang J. Functions and clinical significance of circular RNAs in glioma. *Mol Cancer*. 2020; 19:34.
<https://doi.org/10.1186/s12943-019-1121-0>
PMID:[32061256](https://pubmed.ncbi.nlm.nih.gov/32061256/)
31. Vagia E, Mahalingam D, Cristofanilli M. The Landscape of Targeted Therapies in TNBC. *Cancers (Basel)*. 2020; 12:916.
<https://doi.org/10.3390/cancers12040916>
PMID:[32276534](https://pubmed.ncbi.nlm.nih.gov/32276534/)
32. Mittendorf EA, Zhang H, Barrios CH, Saji S, Jung KH, Hegg R, Koehler A, Sohn J, Iwata H, Telli ML, Ferrario C, Punie K, Penault-Llorca F, et al. Neoadjuvant atezolizumab in combination with sequential nab-paclitaxel and anthracycline-based chemotherapy versus placebo and chemotherapy in patients with early-stage triple-negative breast cancer (IMpassion031): a randomised, double-blind, phase 3 trial. *Lancet*. 2020; 396:1090–100.
[https://doi.org/10.1016/S0140-6736\(20\)31953-X](https://doi.org/10.1016/S0140-6736(20)31953-X)
PMID:[32966830](https://pubmed.ncbi.nlm.nih.gov/32966830/)
33. Patel SP, Kurzrock R. PD-L1 Expression as a Predictive Biomarker in Cancer Immunotherapy. *Mol Cancer Ther*. 2015; 14:847–56.
<https://doi.org/10.1158/1535-7163.MCT-14-0983>
PMID:[25695955](https://pubmed.ncbi.nlm.nih.gov/25695955/)
34. Kingwell K. Neuro-oncology: Glioblastoma prognosis linked to neuronal PD-L1 expression in tumour-adjacent tissue. *Nat Rev Neurol*. 2013; 9:602–3.
<https://doi.org/10.1038/nrneurol.2013.197>
PMID:[24042480](https://pubmed.ncbi.nlm.nih.gov/24042480/)
35. Akram M, Iqbal M, Daniyal M, Khan AU. Awareness and current knowledge of breast cancer. *Biol Res*. 2017; 50:33.
<https://doi.org/10.1186/s40659-017-0140-9>
PMID:[28969709](https://pubmed.ncbi.nlm.nih.gov/28969709/)
36. Jafari SH, Saadatpour Z, Salmaninejad A, Momeni F, Mokhtari M, Nahand JS, Rahmati M, Mirzaei H, Kianmehr M. Breast cancer diagnosis: Imaging techniques and biochemical markers. *J Cell Physiol*. 2018; 233:5200–13.
<https://doi.org/10.1002/jcp.26379> PMID:[29219189](https://pubmed.ncbi.nlm.nih.gov/29219189/)
37. Andrade-Tomaz M, de Souza I, Rocha CR, Gomes LR. The Role of Chaperone-Mediated Autophagy in Cell Cycle Control and Its Implications in Cancer. *Cells*. 2020; 9:2140.
<https://doi.org/10.3390/cells9092140>
PMID:[32971884](https://pubmed.ncbi.nlm.nih.gov/32971884/)
38. Hall A. The cytoskeleton and cancer. *Cancer Metastasis Rev*. 2009; 28:5–14.
<https://doi.org/10.1007/s10555-008-9166-3>
PMID:[19153674](https://pubmed.ncbi.nlm.nih.gov/19153674/)
39. Vakili SA, George A, Ayatollahi SA, Martorell M, Ostrander EA, Salehi B, Martins N, Sharifi-Rad J. Phenolic compounds, saponins and alkaloids on cancer progression: emphasis on p53 expression and telomere length. *Cell Mol Biol (Noisy-le-grand)*. 2020; 66:110–9.
PMID:[32583791](https://pubmed.ncbi.nlm.nih.gov/32583791/)
40. Li G, Hu J, Hu G. Biomarker Studies in Early Detection and Prognosis of Breast Cancer. *Adv Exp Med Biol*. 2017; 1026:27–39.
https://doi.org/10.1007/978-981-10-6020-5_2
PMID:[29282678](https://pubmed.ncbi.nlm.nih.gov/29282678/)
41. Klemm F, Joyce JA. Microenvironmental regulation of therapeutic response in cancer. *Trends Cell Biol*. 2015; 25:198–213.
<https://doi.org/10.1016/j.tcb.2014.11.006>
PMID:[25540894](https://pubmed.ncbi.nlm.nih.gov/25540894/)
42. Deng Z, Wang J, Xu B, Jin Z, Wu G, Zeng J, Peng M, Guo Y, Wen Z. Mining TCGA Database for Tumor Microenvironment-Related Genes of Prognostic Value in Hepatocellular Carcinoma. *Biomed Res Int*. 2019; 2019:2408348.

<https://doi.org/10.1155/2019/2408348>

PMID:[31828095](https://pubmed.ncbi.nlm.nih.gov/31828095/)

43. Wan J, Wang J, Zhou M, Rao Z, Ling X. A cell membrane vehicle co-delivering sorafenib and doxorubicin remodel the tumor microenvironment and enhance immunotherapy by inducing immunogenic cell death in lung cancer cells. *J Mater Chem B*. 2020; 8:7755–65. <https://doi.org/10.1039/d0tb01052a> PMID:[32735004](https://pubmed.ncbi.nlm.nih.gov/32735004/)
44. Zhang W, Shen Y, Huang H, Pan S, Jiang J, Chen W, Zhang T, Zhang C, Ni C. A Rosetta Stone for Breast Cancer: Prognostic Value and Dynamic Regulation of Neutrophil in Tumor Microenvironment. *Front Immunol*. 2020; 11:1779. <https://doi.org/10.3389/fimmu.2020.01779> PMID:[32849640](https://pubmed.ncbi.nlm.nih.gov/32849640/)
45. Zhao Y, Pu C, Liu Z. Exploration the Significance of a Novel Immune-Related Gene Signature in Prognosis and Immune Microenvironment of Breast Cancer. *Front Oncol*. 2020; 10:1211. <https://doi.org/10.3389/fonc.2020.01211> PMID:[32850356](https://pubmed.ncbi.nlm.nih.gov/32850356/)
46. Deng X, Lin D, Chen B, Zhang X, Xu X, Yang Z, Shen X, Yang L, Lu X, Sheng H, Yin B, Zhang N, Lin J. Development and Validation of an IDH1-Associated Immune Prognostic Signature for Diffuse Lower-Grade Glioma. *Front Oncol*. 2019; 9:1310. <https://doi.org/10.3389/fonc.2019.01310> PMID:[31824866](https://pubmed.ncbi.nlm.nih.gov/31824866/)
47. Arora S, Velichinskii R, Lesh RW, Ali U, Kubiak M, Bansal P, Borghaei H, Edelman MJ, Boumber Y. Existing and Emerging Biomarkers for Immune Checkpoint Immunotherapy in Solid Tumors. *Adv Ther*. 2019; 36:2638–78.
48. Xu J, Guo X, Jing M, Sun T. Prediction of tumor mutation burden in breast cancer based on the expression of ER, PR, HER-2, and Ki-67. *Onco Targets Ther*. 2018; 11:2269–75. <https://doi.org/10.2147/OTT.S159830> PMID:[29719409](https://pubmed.ncbi.nlm.nih.gov/29719409/)
49. Cortes J, Cescon DW, Rugo HS, Nowecki Z, Im SA, Yusof MM, Gallardo C, Lipatov O, Barrios CH, Holgado E, Iwata H, Masuda N, Otero MT, et al, and KEYNOTE-355 Investigators. Pembrolizumab plus chemotherapy versus placebo plus chemotherapy for previously untreated locally recurrent inoperable or metastatic triple-negative breast cancer (KEYNOTE-355): a randomised, placebo-controlled, double-blind, phase 3 clinical trial. *Lancet*. 2020; 396:1817–28. [https://doi.org/10.1016/S0140-6736\(20\)32531-9](https://doi.org/10.1016/S0140-6736(20)32531-9) PMID:[33278935](https://pubmed.ncbi.nlm.nih.gov/33278935/)
50. Vonderheide RH, LoRusso PM, Khalil M, Gartner EM, Khaira D, Soulieres D, Dorazio P, Trosko JA, Rüter J, Mariani GL, Usari T, Domchek SM. Tremelimumab in combination with exemestane in patients with advanced breast cancer and treatment-associated modulation of inducible costimulator expression on patient T cells. *Clin Cancer Res*. 2010; 16:3485–94. <https://doi.org/10.1158/1078-0432.CCR-10-0505> PMID:[20479064](https://pubmed.ncbi.nlm.nih.gov/20479064/)
51. Ott PA, Hodi FS, Kaufman HL, Wigginton JM, Wolchok JD. Combination immunotherapy: a road map. *J Immunother Cancer*. 2017; 5:16. <https://doi.org/10.1186/s40425-017-0218-5> PMID:[28239469](https://pubmed.ncbi.nlm.nih.gov/28239469/)

SUPPLEMENTARY MATERIALS

Supplementary Tables

Supplementary Table 1. siRNA sequences for POP1.

Gene	Sense 5'-3'	Antisense 5'-3'
si-NC	CAGAAGAATGGTACAAATCCAAG	CTTCG TTCAGTATGTTAATCGT
si-POP1-1	GCAGTGCATTCTCAGTATA	TATACTGAGAATGCACTGC
si-POP1-2	GCTCGAAGATGTCACATGA	TCATGTGACATCTTCGAGC
si-POP1-3	GCAGGAAGCTCTGACTCTA	TAGAGTCAGAGCTTCCTGC

Supplementary Table 2. Primers for qRT-PCR.

mRNA	Species	Forward	Reverse
POP1	Human	AGAGGTGTAAAGCACACAGT	GCTGTCGTGAAGTTCAGG
GAPDH	Human	GGAGCGAGATCCCTCCAAAAT	GGCTGTTGTCATACTTCTCATGG